Photoproduction of Neutral Pions from Hydrogen at Forward Angles from 240 to 480 Mev*

W. S. McDONALD AND V. Z. PETERSON, *California Institute of Technology, Pasadena, California*

AND

D. R. CORSON, *Cornell University, Ithaca, New York*

(Received March 25, 1957)

Recoil protons from the process $\gamma+p\rightarrow p+\pi^0$ have been detected by nuclear emulsions placed within a hydrogen-gas target and used to measure the differential cross section for production of neutral pions. In this manner protons of energies as low as 5 Mev can be detected at laboratory angles corresponding to emission of a pion at center-of-momentum (c.m.) angles as low as 26°. This experiment thus supplements that of Oakley and Walker which is in the same range of photon energies (240–480 Mev), but is restricted to pion c.m. angles greater than about 70° owing to higher minimum detectable proton energy. Common experimental points provide intercomparison of absolute values. Angular distributions are analyzed in the form $d\sigma/d\Omega=A+B\cos\theta+C\cos^2\theta$ in the c.m. system. The combined Oakley-Walker and present data give the average value of the ratio A/C as -1.60 ± 0.10 in the energy range from 260 to 450 Mev. The coefficient B, which gives the front-back asymmetry, passes through zero below the resonance energy of 320 Mev and is positive at higher energies. These results are consistent with magnetic dipole absorption leading to a state of the pion-nucleon system of angular momentum $\frac{3}{2}$, together with a finite amount of S-wave interference.

I. INTRODUCTION

THE differential cross section for the photoproduction of neutral pions at forward angles from hydrogen by photons in the energy interval from 240 to 480 Mev has been measured by means of nuclear emulsions. These measurements extend the angular distribution measured in this laboratory (Synchrotron Laboratory, California Institute of Technology) by Oakley and Walker[1] who used a magnetic spectrometer and counter system to measure the cross section from 70° to 153° in the center-of-momentum (c.m.) system. Oakley and Walker detected the recoil proton emitted in the reaction,

$$\gamma+p\rightarrow p+\pi^0.$$

The lower limit on pion angles (70° in the c.m. system) which they could measure was set by the lowest-energy proton which their counters could detect. Self-absorption in the target and counters set this low-energy limit at about 25 Mev. In order to measure the energy and angular distributions of recoil protons of lower energy, nuclear emulsions were placed inside a hydrogen-gas target. The minimum detectable recoil-proton energy (5 Mev) was, therefore, limited only by the range in the target gas. This enabled differential cross section measurements for pion angles as low as 26° (c.m.).

If differential cross sections, $d\sigma/d\Omega$, at a given photon energy and various pion c.m. angles, θ, are fitted to a formula of the type

$$d\sigma/d\Omega=A+B\cos\theta+C\cos^2\theta, \quad (1)$$

the coefficients A, B, and C may be calculated at that energy. This assumes production in S- and P-states only. In this paper the new results are taken together with those of Oakley and Walker and new A, B, and C coefficients are computed in the energy range from 260 to 450 Mev. The same beam monitor was used in both experiments, and the results of both experiments agree with each other within experimental error in the region near $\theta=90°$, where they overlap. The value of the A coefficient, which is determined by the cross section at 90°, is changed but little. However, the addition of new results of comparable statistical weight at forward angles makes possible a more accurate determination of the B and C coefficients than is possible from data which is restricted to essentially the backward hemisphere only.

II. EXPERIMENTAL PROCEDURE

The experimental apparatus is shown in Fig. 1. This arrangement is similar in principle to that of Goldschmidt-Clermont, Osborne, and Scott[2] who measured neutral-pion differential cross sections for gamma-ray energies from 170 to 340 Mev with nuclear emulsions.

The 500-Mev bremsstrahlung beam of the California Institute of Technology electron synchrotron passed through a tapered lead collimator and secondary beam "scraper" into the hydrogen tank through a 0.019-in. stainless steel window and out through a 0.031-in. stainless steel exit window. It was found necessary to make the target tank quite long in order to keep the entrance window and emulsion chamber well separated from each other and hence to prevent excessive electron background produced in the entrance window from blackening the emulsions. Background electrons produced in the windows were deflected by a 10 000 gauss

* This work was supported by the U. S. Atomic Energy Commission.

[1] D. C. Oakley and R. L. Walker, Phys. Rev. **97**, 1283 (1955).

[2] Goldschmidt-Clermont, Osborne, and Scott, Phys. Rev. **89**, 329 (1953); **97**, 188 (1955).

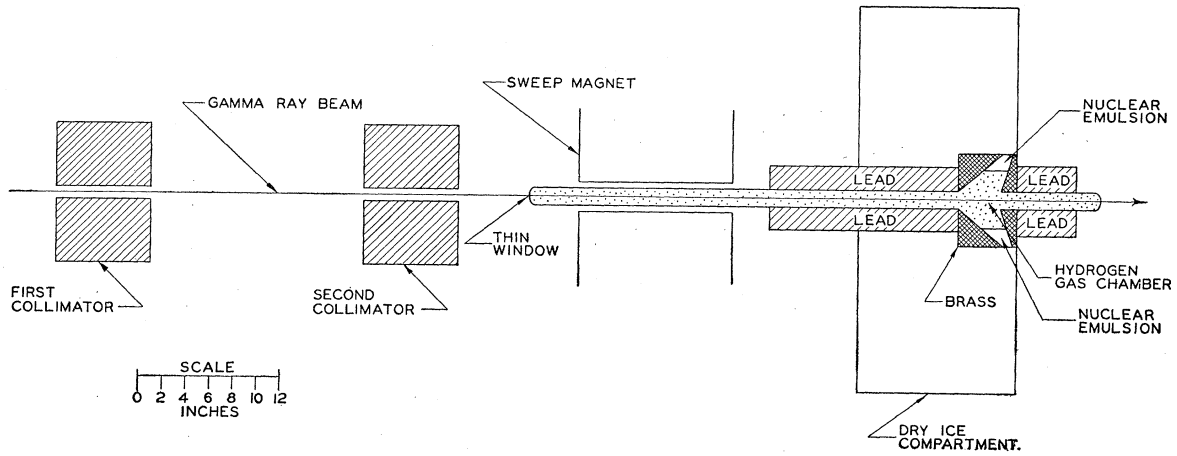

FIG. 1. Schematic diagram of the experimental arrangement of emulsion pellicles in the hydrogen gas target.

magnetic field and absorbed in thick lead walls surrounding the entrance tube (see Fig. 1). The total exposure was 3.84×10^{14} Mev as measured by the same monitor ionization chamber used by Oakley and Walker[1] (hereafter referred to as O.W.).

The hydrogen was cooled by a dry ice and alcohol mixture held in a Styrofoam-insulated compartment enclosing the target. The average hydrogen-gas pressure was 367 psi. Due to a leak in the target tank the gas pressure varied from 440 to 240 during the exposure. An accurate time-pressure record was kept during the run and the error in the integrated (density×exposure) value is estimated to be less than 3%. The variation in gas pressure also produces an uncertainty of about ±50 microns (emulsion equivalent) in the proton hydrogen range. Fortunately, this does not seriously affect the resolution in range required to define the cross sections.

Nuclear emulsions exposed to hydrogen gas at room temperature for a few minutes will be badly blackened when developed because of reduction of the AgBr. The temperature coefficient of this reaction is such that hydrogen at dry-ice temperature produces no blackening after many hours exposure. Cooling the gas, therefore, has the dual purpose of preventing emulsion blackening and increasing the gas density.

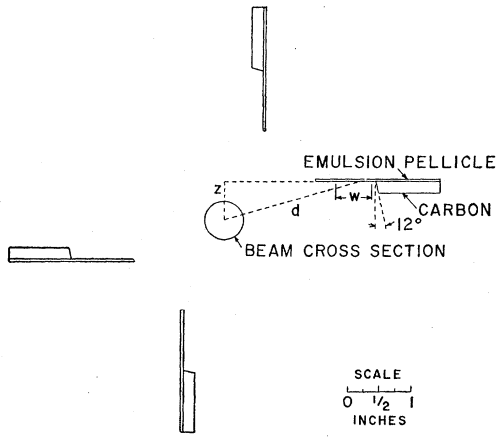

FIG. 2. Schematic diagram of the emulsion geometry looking directly into the beam.

The brass emulsion chamber held two pairs of 600-micron *C2* pellicles placed on opposite sides of the beam center-line (see Fig. 2). A similar emulsion geometry was used by Panofsky and Fillmore.[3] This geometry has the advantage that if the measurement of cross section is based on the *sum* of the tracks measured in paired plates, any error due to an error in beam centering is reduced. The beam was carefully centered and its diameter (19/32 in.) measured with x-ray film. The distribution in dip angle of tracks found in each pellicle was also in agreement with a well-centered beam.

Pellicles were used instead of glass-backed emulsions because it was found that emulsion bonded to glass cracked when exposed to the cold hydrogen gas. One pellicle at each of the four positions around the beam was sufficient to stop protons in the low-energy range under investigation. This made it possible to avoid the time-consuming operation of tracing tracks through a pellicle stack. Since the protons were required to stop in the emulsion, range was used to determine the energy.

As a check on the normalization of this experiment relative to that of O.W., we have measured some cross sections already measured by them. To accomplish this, it was necessary to stop protons of a higher energy in the emulsion than could be stopped with a single pellicle. Therefore, protons of higher energy were slowed down by a carbon absorber placed over the rear portion of each pellicle. Protons passing through the front, bevelled edge of the carbon absorber and stopping in the emulsion constitute the high-energy or "under carbon" data of the experiment.

[3] W. K. H. Panofsky and F. L. Fillmore, Phys. Rev. **79**, 57 (1950).

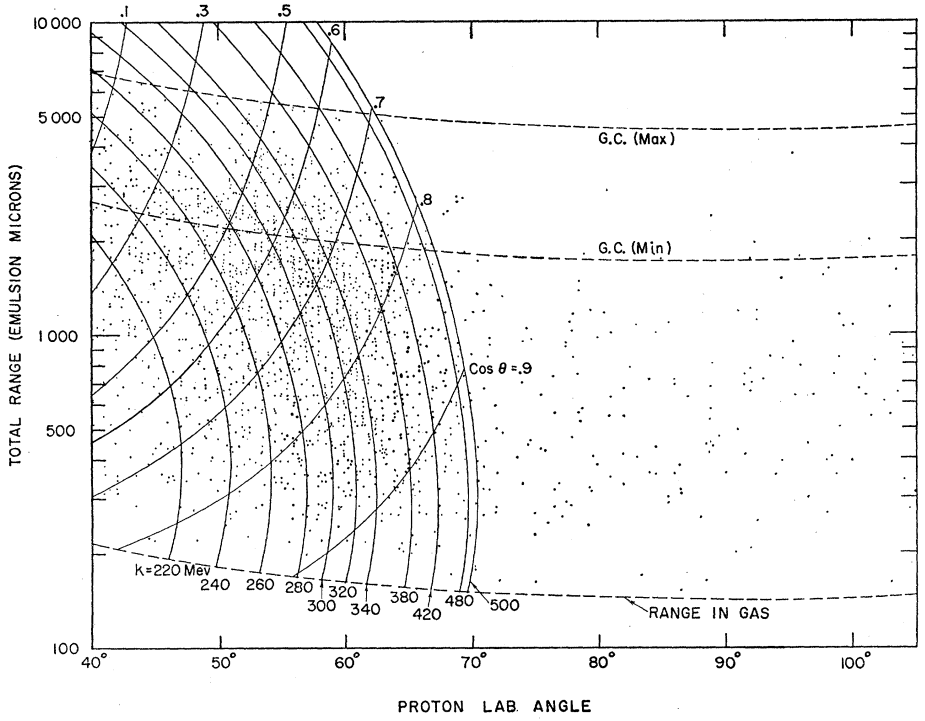

FIG. 3. Typical range *vs* angle plot of protons ending in a 600-micron pellicle. The solid lines denote constant photon energy and pion c.m. angle. The dashed lines are limiting ranges (see text). This plot represents 58% of the total "bare emulsion" data.

After processing, one pair of emulsions was sent to Cornell for scanning and the other was scanned by the CalTech emulsion group. The plates were scanned for proton endings and each track was traced back to the point at which it entered the emulsion surface. The scanning was done using 55× oil-immersion objectives and 15× flat-field eyepieces. The visual appearance of each track was sufficient to distinguish protons from the stopping charged pions in the emulsion. Identifying protons at the end of their range makes the scanning efficiency energy-independent, since all track endings have the same appearance.

The projected range as well as the projected angle and the dip angle of each track at the emulsion surface was measured. The first 100 microns of track was used to measure angles. From these data the polar angle of emission and initial residual range of the proton were computed. The range is estimated to be accurate to within $\pm 2\%$, and the measured angles to ± 0.3 degree. These data also made it possible to project back each track to see that its emulsion trajectory was consistent with the hypothesis that the track came from the direction of the beam. This procedure permitted discrimination against background protons, such as cosmic-ray protons, produced by reactions taking place outside of the hydrogen gas. Projecting back each track also gave its range in the hydrogen gas.

In the case of the "under carbon" tracks which had passed through the bevelled front edge of the carbon absorber, it can be shown that the range in carbon, neglecting scattering, is determined only by the distance back from the front edge of the absorber that the track enters the emulsion and does not depend upon the dip angle of incidence of the track upon the absorber. This is true because the bevel angle was chosen so that all protons from the beam striking the absorber would be in a plane essentially normal to the absorber. Emulsion ranges were related to proton energy using the range-energy relation of Fay, Gottstein, and Hain.[4] Hydrogen and carbon ranges were taken from the range-energy relations of Aron, Hoffman, and Williams.[5]

Each track was recorded on a kinematic plot, an example of which is shown in Fig. 3. This plot represents 58% of the total "bare emulsion" data, i.e., data not including tracks which passed through the carbon absorber. Each point represents one proton track. The range in gas is included and is expressed in microns of emulsion equivalent. The solid curved lines in Fig. 3 are lines of constant photon energy, k, and of constant $\cos\theta$, where θ is the pion c.m. angle. The data are thus presented in convenient form for computing cross sections. The center-of-momentum differential cross section, $d\sigma/d\Omega$, for photoproduction of π^0 mesons at an angle θ by photons of energy k is

$$Y=(d\sigma/d\Omega)nN(k)\,\Delta k\,\Delta(\cos\theta)\,(LWZ/d^2), \qquad (2)$$

where Y is the yield of protons from the π^0 reaction in the photon energy interval Δk and $\cos\theta$ interval

[4] Fay, Gottstein, and Hain, Suppl. Nuovo cimento **11**, No. 2, 234 (1954).

[5] Aron, Hoffman, and Williams, U. S. Atomic Energy Commission Report AECU-663 (unpublished).

$\Delta(\cos\theta)$. $N(k)$ is the number of photons per unit photon-energy interval at the photon energy k (lab system), and n is the number of hydrogen atoms per cm^3. L is the length (parallel to the beam) of the area scanned, which is also the effective target length. W is the width of the area scanned. Z is the offset distance from the beam center to the plate, and d is the perpendicular distance from the beam center-line to the center of the scan area (see Fig. 2). Measuring Z and d from the beam center rather than integrating over the finite beam diameter introduces an uncertainty of no more than 1% in the effective solid angle.

It was necessary to take the finite beam size into account, however, in order to obtain cross sections in the high-proton-energy region of the "bare emulsion" data. This is because the maximum range a proton may have in the emulsion, depends upon the dip angle at which it enters the emulsion surface, and hence on the distance from the beam center line of the proton's point of origin. The dashed horizontal lines in the upper part of Fig. 3 show this effect, the upper and lower lines corresponding to protons having the minimum and maximum possible dip angles, respectively. Kinematic intervals were chosen in computing cross sections so that the correction necessary for this "finite-beam effect" did not exceed 6%. Four of the cross sections listed in Table I were so corrected.

III. BACKGROUND

For protons produced in the reaction

$$\gamma+p\rightarrow p+\pi^0$$

by 500-Mev bremsstrahlung, the maximum laboratory angle of emission is about 71°. Figure 3 shows protons at angles greater than this. A few of these events may be accounted for as π^0 protons scattered by the hydrogen and emulsion into the angular region beyond the kinematic cutoff. The bulk of these events, however, is due to reactions other than the π^0 reaction, and it is necessary to correct the π^0 cross sections by taking these reactions into account. There are a number of possible sources of background, which are discussed below.

TABLE I. Forward angular distribution in the c.m. system, $d\sigma/d\Omega$, in units of 10^{-30} cm^2/sterad. "Bare emulsion" data only.

Photon energy (lab) (Mev)	Pion angle (c.m.) $\cos\theta$	Mean θ	$d\sigma/d\Omega$
260 (240–280)	0.8–0.7	41.3°	9.5±1.0
260 (240–280)	0.7–0.5	52.8°	9.9±0.8
300 (280–320)[a]	0.9–0.8	31.4°	10.7±1.2
300 (280–320)[a]	0.8–0.7	41.3°	16.1±1.4
320 (300–340)[a]	0.9–0.8	31.4°	17.2±1.6
320 (300–340)[a]	0.8–0.6	45.0°	21.3±1.4
360 (340–380)	0.9–0.8	31.4°	14.8±1.5
360 (340–380)	0.8–0.7	41.3°	15.6±1.6
400 (380–420)	0.9–0.8	31.4°	10.2±1.2
450 (420–480)	0.9–0.8	31.4°	6.7±1.0

[a] Overlapping data regrouped to allow direct comparison with the data of Oakley and Walker (reference 1).

A. Protons from Sources Outside the Gas

Although x-ray pictures taken of the collimated beam show ample clearance between the beam and the collimators, we have sought further evidence of background from the lead or brass surrounding the chamber. If a portion of the beam struck one side of the shielding, the background yield would be expected to vary from plate to plate. However, the background per unit solid angle is the same, well within statistics, for each of the four plates. Hence, we consider this source of background unlikely. A uniformly-irradiated-shielding source of background also seems unlikely. The trajectory of each track was traced back to see if it came from the target region where the beam was striking the gas. About 12% of all protons entering the emulsion surface appeared to come from areas other than the bombarded gas. These can all be accounted for as cosmic-ray tracks present in the emulsion and are qualitatively similar to the tracks found in an unexposed control plate of the same emulsion batch.

B. Protons from Pion Pair Production

The maximum laboratory angle that a proton from the reactions

$$\gamma+p\rightarrow p+\pi^+ +\pi^-,\quad \gamma+p\rightarrow p+\pi^0+\pi^0,$$

can come out at is 47 degrees, where the photon energy is 500 Mev. This angle is outside the angular interval from which the cross section data were taken.

C. Compton Effect

Compton-recoil protons may be produced in the c.m. angular interval from 0 to 90°. Recent experimental results[6] show that the Compton proton cross section may be as high as 15 times the Thomson cross section. Such a cross section would produce a proton contribution amounting to less than 3% of the total protons observed.

In order to be detected in the present experiment, a proton must have an energy of at least 5 Mev, corresponding to a c.m. angle of 81° for a Compton proton produced by a 500-Mev gamma ray. Compton protons may therefore be present in the angular region between 71° and 81° beyond the π^0-proton kinematic angular limit. The background in this angular region is slightly larger than that at angles beyond 81° but this effect can be completely accounted for by the scattering of π^0 protons into the 71° and 81° interval. Detection of the Compton effect is therefore beyond the resolution of the present experiment because it is masked at angles beyond the π^0 kinematic limit by scattered π^0 protons

[6] T. Yamagata, Ph.D. thesis, University of Illinois, 1956 (unpublished).

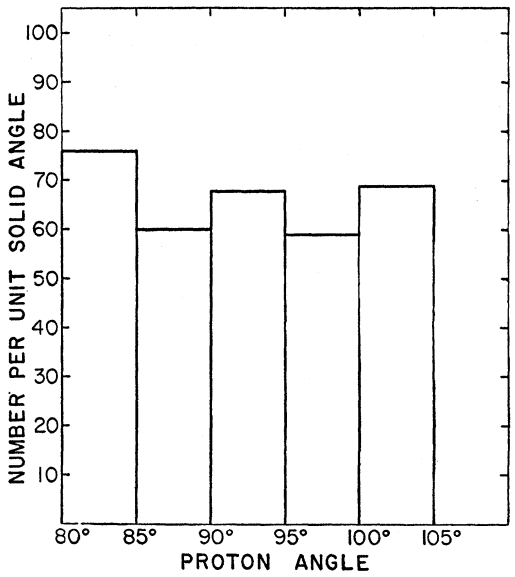

FIG. 4. Histogram showing the angular distribution (in the laboratory system) of background protons of energy less than 20 Mev at laboratory angles between 80° and the geometrical cutoff angle of 105°.

and the background which in the next section is shown to be due to impurities in the gas.

D. Protons from Impurities in the Gas

The histogram in Fig. 4 shows the angular distribution of background protons with energy less than 20 Mev at laboratory angles between 80° and 105°. The latter angle is the minimum geometrical cutoff angle defined by the shielding. Protons from the π^0 reaction have little chance of being scattered into this angular region, so that the protons in this region must come from other processes. As shown in Fig. 4, the angular distribution is consistent with isotropy. The energy spectrum of these background protons is measured to obey an $E^{-1.6\pm0.3}$ law, where E is the proton energy. Levinthal and Silverman[7] have measured the angular distribution and energy spectrum for protons from 7 to 70 Mev produced by 320-Mev bremsstrahlung on carbon. They found an isotropic angular distribution for 10-Mev protons and an energy spectrum of the form E^{-S}, where $S=1.7\pm0.1$ for carbon and varies slowly with atomic number. Absolute photoproton-production cross sections for nuclei exposed to 300-Mev bremsstrahlung were measured by Keck.[8] Study of photostars produced by 500-Mev bremsstrahlung[9] indicates that Keck's cross sections may be extrapolated to 500 Mev by multiplying them by a factor of 2.5.

Upon using these results, the observed background angular distribution, energy spectrum, and magnitude can all be accounted for by a nitrogen impurity of 0.17 mole percent in the hydrogen gas of the target. An analysis of the actual gas used in the target was not made, but this impurity figure is consistent with the values found by mass spectrographic analyses of hydrogen from the same tank used both prior to, and after, the experimental run. The background protons were therefore attributed to reactions with the nuclei of the impurities, mostly nitrogen, as was found to be the case in the similar emulsion experiment of Goldschmidt-Clermont, Osborne, and Scott.[2] The π^0 cross sections were corrected by subtracting the background contribution assuming an isotropic angular distribution and an $E^{-1.7}$ energy spectrum. In the energy interval in which the bulk of the background is found the assumption of angular isotropy is an excellent one. At higher energies, approaching 40 Mev, where the photoproton angular distribution begins to show a forward peaking, the background becomes negligible because of the rapid falloff with proton energy. The background correction varies between 5% and 32% and averages 15%.

[7] C. Levinthal and A. Silverman, Phys. Rev. **82**, 822 (1951).
[8] J. C. Keck, Phys. Rev. **85**, 410 (1952).
[9] V. Z. Peterson and C. E. Roos, Phys. Rev. **105**, 1620 (1957).

IV. CORRECTIONS AND UNCERTAINTIES

The uncertainties in the experiment may be divided into three types: those affecting only the absolute cross section, those affecting the relative cross sections, and random statistical uncertainties.

A. Uncertainties Which Affect the Absolute Cross Section

1. Absolute beam monitor calibration.—This is estimated to be 7%, as discussed in reference 1, and is *not* included in the uncertainties assigned to the cross sections in Table I.

2. *Average target gas density.*—This is estimated at 3% and is included in the assigned uncertainties.

3. Scanning efficiency.—This was measured by duplicate scanning and was found to be $95\pm2\%$ on three of the plates contributing a total of 1288 events used in the cross section calculations (see Table II). On the fourth plate the scanning efficiency was $75\pm3\%$, the reduced efficiency being attributed to a darkening of the emulsion during processing. A total of 237 events were used from this last plate, giving a grand total of 1525 events from all four plates. The cross sections have been corrected for these efficiencies and the scanning-efficiency uncertainty is included in the uncertainty assigned to the cross sections.

TABLE II. Summary of the "bare emulsion" experimental data.

Plate	Area scanned (cm²)	Scanning efficiency (%)	Number of events	Laboratory scanned
1	0.90	95±2	144	CalTech
2	2.74	95±2	388	CalTech
3	5.71	95±2	756	Cornell
4	2.26	75±3	237	Cornell

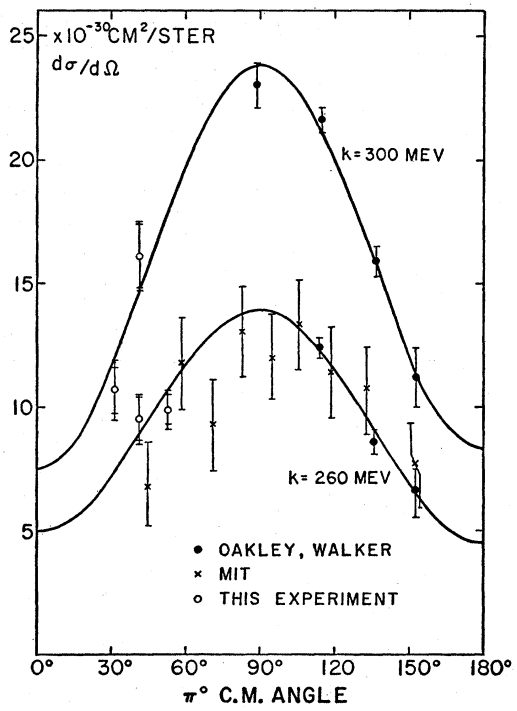

FIG. 5. Angular distributions (in the center-of-momentum system) for photon energies (lab system) of $k=260$ Mev and 300 Mev. The open circles are the present results and the solid circles are the results of Oakley and Walker. The crosses are the 260-Mev results of Goldschmidt-Clermont, Osborne, and Scott. The solid curves are least-squares fits to the combined Oakley and Walker and present data under the assumption that $\sigma(\theta)=A+B\cos\theta+C\cos^2\theta$. Two uncertainties are shown for the present experimental points, the "inside" uncertainties representing standard deviations due to statistics only, and the "outside" uncertainties are the total standard deviations.

4. Geometrical uncertainties.—Uncertainties due to beam-centering[3] and measuring of geometrical distance have been estimated as less than 2% and are included in the assigned uncertainty. A $1\frac{1}{2}$% correction for the measured solid angles was made to take account of emulsion contraction due to exposure at a temperature less than that at which the emulsions were scanned.

B. Uncertainties Which Affect the Relative Cross Sections

1. Background.—The background correction varies from 5% to 32% with an average value of 15%. This correction is based on 190 events and believed accurate within 15%. Therefore, the background introduces an uncertainty which varies from less than 1% to about 5%. This uncertainty is included in the uncertainty assigned to the cross sections.

2. Uncertainty in proton range and angle.—The emulsion range measurements are estimated to be accurate within ± 2%. The variation in hydrogen-gas pressure introduces an additional uncertainty of ± 50 microns of emulsion equivalent. The uncertainty in reading the proton angle is about 0.3°. This is smaller than the angular uncertainty due to scattering in the gas and emulsion, which is estimated to have a root mean square spread varying from $\pm 3°$ to $\pm 1°$ for protons of 400 to 2000 microns total range (emulsion equivalent). If all proton ranges and angles were actually in error by an amount equal to the value of the estimated uncertainties, then the error introduced in the pion c.m. angles for the cross sections listed in Table I would be about 1°, and the error in photon energy would vary from 10 to 30 Mev with an average of 20 Mev. The density of events in Fig. 3 varies slowly enough so that scattering introduces negligible correction to the cross section except near the kinematic limit, where the density varies abruptly. The 450-Mev point is the only point requiring a correction, which is calculated to be 12 ± 6%, the assigned uncertainty being due to the uncertainty in the rms scattering angle of the proton.

C. Random Statistical Uncertainties

These are the counting statistics and are shown for the present experimental points as the inner uncertainties in Figs. 5–7. The statistical uncertainties shown are standard deviations.

Since our data are most useful when combined in an angular distribution with the data of O.W., we have shown those uncertainties which affect our data relative to theirs. This includes all but the beam-monitor-calibration uncertainty, and is typically 10%.

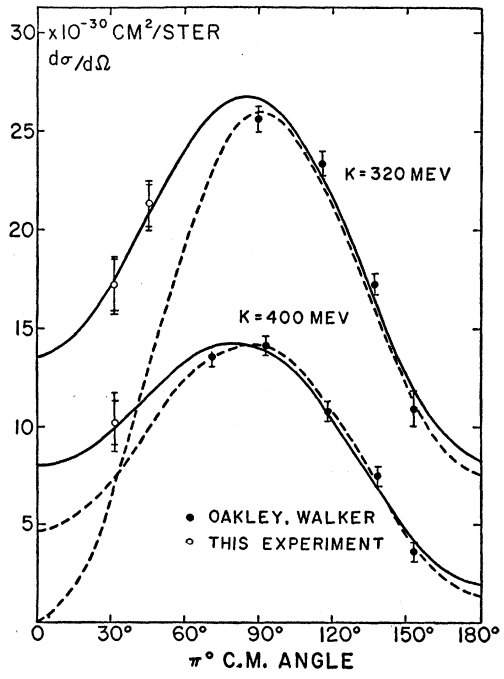

FIG. 6. Angular distributions (c.m.) for $k=320$ Mev and 400 Mev. The solid lines are least-squares fits to the combined Oakley and Walker data and present data. The dashed lines are least-squares fits to the Oakley and Walker data only.

V. DIFFERENTIAL CROSS SECTIONS COMPARED WITH OTHER DATA

The differential cross sections for the "bare emulsion" data are given in Table I. These cross sections are based on the data tabulated for each of the four plates in Table II. In Table III are summarized the "under carbon" cross sections selected to overlap previous measurements of O.W. The weighted average of the ratio of the cross sections of Table III to the corresponding ones of O.W. is 1.02±0.09. Because of this agreement between the two experiments, we have not normalized the absolute values obtained in this experiment.

Differential cross sections for mean photon energies of 260, 300, 320, 360, 400, and 450 Mev are shown in Figs. 5–7. The solid points are the measurements of O.W. and the open points are the present measurements. Actually O.W. made measurements at 270 and 295 Mev. The excitation functions given by them have been used to calculate cross sections at 260 and 300 Mev in order to compare directly with the present work. The solid curves of Figs. 5, 6, and 7 are least-squares fits to the observed data from both experiments, when one assumes an angular distribution in the form of Eq. (1). The dashed curves of Figs. 6 and 7 are drawn from the A, B, and C coefficients given by O.W.,[10] based on their data only. It is clear that the new measurements have made significant changes in the angular-distribution coefficients. These changes are particularly evident at energies near resonance where the cross sections at forward angles predicted by the O.W. angular-distribution coefficients fall well below the measured values. This reflects the fact that accurate determination of the B and C coefficients requires data at both forward and backward angles.

Goldschmidt-Clermont *et al.*[2] have measured π^0 cross sections at the Massachusetts Institute of Technology for gamma-ray energies from 170 Mev to 340 Mev. The absolute normalization of the results quoted by them is based on the adjustment of their monitor calibration

TABLE III. "Under-carbon" differential cross sections (c.m.) compared to Oakley and Walker values. $d\sigma/d\Omega$ in units of 10^{-30} cm²/sterad.

Mean photon energy (lab) k (Mev)	Mean angle (c.m.) θ	No. of events	$d\sigma/d\Omega$	Oakley and Walker $d\sigma/d\Omega$	Ratio
300	87°	83	23.2	23.5	0.99±0.13
320	80°	63	20.0	25.0	0.80±0.15
360	60°	60	23.4	18.0	1.30±0.18
				Average ratio =	1.02±0.09

[10] These A, B, and C coefficients are taken from the solid curve of Fig. 9 of reference 1. The requirement that the cross section remain positive at all angles has influenced their choice of B and C at 320 Mev to values more positive than that indicated by their data alone. With the new coefficients, obtained by least-squares fit, no difficulty with negative cross sections is encountered.

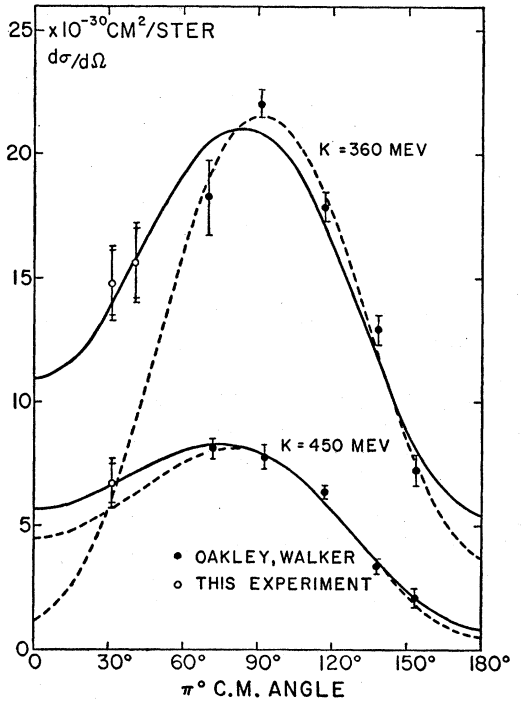

FIG. 7. Angular distributions (c.m.) for k=360 Mev and 450 Mev. The solid curves are least-squares fits to the combined Oakley and Walker data and the present data. The dashed lines are least-squares fits to the Oakley and Walker data only.

to agree with monitor calibrations of the Cornell Synchrotron and Illinois Betatron laboratories which are in mutual agreement. The beam monitor calibration at the CalTech Synchrotron Laboratory is such that on this basis alone the absolute cross sections measured by O.W. and the present experiment would be 5% lower than those measured at Cornell and Illinois[11] (and therefore at MIT). Above 280 Mev the cross sections given by Goldschmidt-Clermont *et al.* are considerably lower than the O.W. results, a fact which is perhaps due to the difficulties in obtaining data so near the upper end of the MIT bremsstrahlung spectrum. The MIT results in the energy interval k=240–280 Mev are included in Fig. 5, along with the present data and the O.W. data. The agreement seems reasonably good.

VI. ANGULAR DISTRIBUTION COEFFICIENTS

The final A, B, and C coefficients are listed in Table IV and plotted in Fig. 8 as a function of photon energy. The solid curves for A, B, and C are a visual fit to the present results and at low energies are drawn to fit the recent Illinois results of Koester and Mills.[12]

The dashed curves for A and C in Fig. 8 are the experimental values of A^0 and C^0 adopted in the partial-

[11] Walker, Teasdale, Peterson, and Vette, Phys. Rev. **99**, 210 (1955).

[12] L. J. Koester and F. E. Mills, Phys. Rev. **105**, 1900 (1957). The authors wish to thank Dr. Koester and Dr. Mills for communicating these results prior to publication.

TABLE IV. A, B, and C coefficients in units of 10^{-30} cm²/sterad.

k (Mev)	260	300	320	360	400	450
A	13.9 ±0.7	23.8 ±0.7	26.6 ±0.6	20.9 ±0.7	14.1 ±0.4	8.0 ±0.5
B	0.2 ±0.6	−0.4 ±0.7	2.7 ±0.8	2.7 ±0.7	3.0 ±0.7	2.4 ±0.6
C	−9.2 ±1.7	−15.9 ±1.4	−15.6 ±1.3	−12.8 ±1.4	−9.1 ±1.1	−4.7 ±0.8
$-A/C$	1.52±0.29	1.50±0.14	1.70±0.15	1.64±0.19	1.55±0.19	1.69±0.28
	Average value of $A/C=-1.60\pm0.10$					

wave analysis of the photomeson cross sections by Watson, Keck, Tollestrup, and Walker.[13] Their choice of A^0 and C^0 was based on the experimental results of O.W. at high energy (above 290 Mev) and fits fairly well the results of Goldschmidt-Clermont *et al.*[2] below this energy. Older π^0 experiments which were not given as much weight by Watson *et al.* in their analysis were those of Silverman and Stearns[14] and Walker, Oakley, and Tollestrup.[15] The dashed curve for B is that given by O.W. and is based on their data and the MIT[2] data. Since the value of B depends on the front-to-back ratio, the error for this coefficient is rather large in the O.W. experiment.

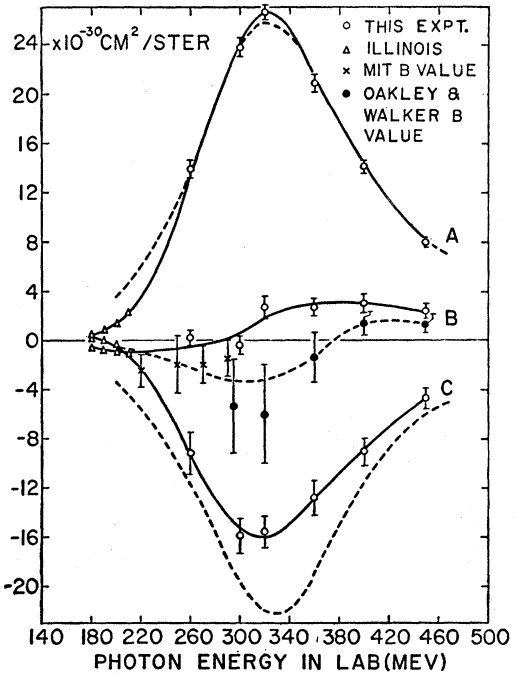

FIG. 8. Coefficients of the c.m. angular distribution $d\sigma_{\text{c.m.}}/d\Omega = A+B\cos\theta+C\cos^2\theta$ plotted as a function of photon energy in the laboratory system. The dashed curves for A and C are the experimental values of A and C adopted by Watson *et al.* (reference 13). The dashed curve for B is that given by Oakley and Walker (reference 1) and is a fit to their data for B and the MIT B data (reference 2). The solid curves for A, B, and C are visual fits to the present results and the Illinois data (reference 12).

[13] Watson, Keck, Tollestrup, and Walker, Phys. Rev. **101**, 1159 (1956).
[14] A. Silverman and M. Stearns, Phys. Rev. **88**, 1225 (1952).
[15] Walker, Oakley, and Tollestrup, Phys. Rev. **97**, 1279 (1955).

Above 260 Mev it is clear that the present results have not changed A appreciably, but that C has become considerably less negative. The ratio A/C from 260 to 450 Mev is changed to an average value -1.60 ± 0.10 as contrasted to the value -1.22 ± 0.10 obtained by O.W. If neutral pions were produced only by magnetic dipole absorption leading to a state of angular momentum $J=\frac{3}{2}$, then the ratio of A/C would be $-5/3=-1.67$ which is consistent with the new experimental value.

A pure magnetic dipole interaction would imply that $B=0$. However, the solid curve for B in Fig. 8 shows that B becomes positive somewhat below resonance and is definitely positive at energies above resonance. The nonzero value for the interference term, B, above resonance, indicates a finite amount of S-wave production in this energy region.

Arguments for the existence of S-wave production (i.e., nonzero values of B) at low energies have been given by Koester and Mills,[12] in analyzing their total cross section and 135° differential cross section measurements. The assumption that $B=0$ leads them to deduce values of A/C in violent disagreement with the theory of Chew and Low,[16] whereas the magnetic dipole value

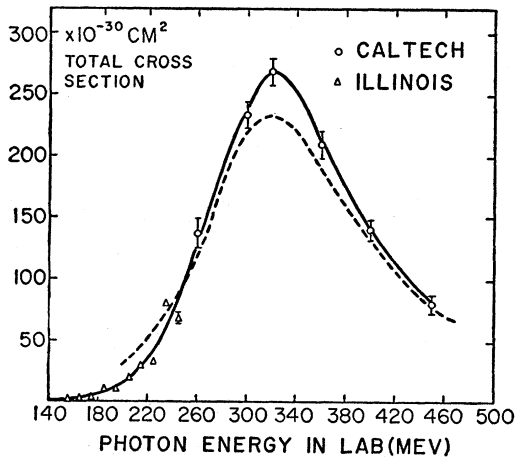

FIG. 9. Total cross sections (in the center-of-momentum system) as calculated from the A and C coefficients given by the solid and dashed curves in Fig. 8, except that below 245 Mev the solid curve is that given by Koester and Mills (reference 12) from their measurements of the total cross section.

[16] G. F. Chew and F. E. Low, Phys. Rev. **101**, 1570 (1956); **101**, 1579 (1956).

of $A/C=-5/3$ requires B to become so negative as to give negative 0° cross sections. They conclude that finite negative values of B are required below about 210 Mev. In Fig. 8 we have plotted the Illinois values of A, B, and C obtained by assuming that the zero-degree cross section is actually zero ($A+B+C=0$). When calculated in this manner, the coefficient C becomes positive at about 190 Mev (see Fig. 8) and the curves for B and C cross each other near 205 Mev. The magnitudes of A and C are substantially smaller than those based on the MIT[2] data.[17]

[17] *Note added in proof.*—Since the writing of this paper, the present experimental results have been compared with some recent theoretical work of Professor Chew and his collaborators [Chew, Goldberger, Low, and Namber, Phys. Rev. (to be published)]. This theory relates pion photoproduction to pion-nuclear scattering through the experimentally determined scattering phase shifts. Good agreement between the present A, B, and C coefficients and the theoretical coefficients is obtained at all energies from resonance to 450 Mev. The value at which the B coefficient crosses the zero axis (about 280 Mev) is also in good agreement with theory. In making the comparison all P wave scattering phase shifts except δ_{33} were taken to be zero. The values of δ_{33} used were those summarized by Ashkin *et al.* [Ashkin, Blaser, Feiner, and Stern, Phys. Rev. **105**, 724 (1957)] below pion laboratory kinetic energies of 220 Mev, and the Russian results [E. L. Gregoriev and N. A. Mitin, Soviet Phys. JETP 4, 10 (1957)] at 310 Mev. The S-wave phase shifts used, δ and δ_3, were obtained by linear extrapolation from the low energy slopes [J. Orear, Phys. Rev. **100**, 288 (1955)]. The value of the coupling constant used was $f^2=0.08$, which was obtained from the scattering experiments. It is of interest to note that the theory assumes only dipole radiation and no electric quadrupole term is included. The authors wish to thank Professor Chew for communicating the new results prior to publication.

The uncertainties assigned to the A, B, and C coefficients above 260 Mev are based on the uncertainties assigned to the O.W. and present differential cross sections. If the ratio of the present results to those of O.W. were in error by 9% owing to an error in our absolute scale (see Table III), the values of the B and C coefficients would change by about the uncertainty shown in Fig. 8.

VII. TOTAL CROSS SECTIONS

Total cross sections (in the center-of-momentum system) are shown in Fig. 9. The solid curve below 245 Mev is drawn to fit the total cross sections measured by Koester and Mills.[12] The solid curve above 245 Mev and the dashed curve are obtained from the respective A and C curves in Fig. 8 by means of the formula

$$\sigma_T=4\pi(A+\tfrac{1}{3}C), \tag{3}$$

where σ_T is the total cross section and the formula is obtained by the integration of Eq. (1).

ACKNOWLEDGMENTS

The careful scanning of the plates was largely the work of Mrs. Hedva Forman, Mrs. Elaine Motta, Mrs. Carol Sienko, and Mrs. Jane Loeffler.

We wish to thank Dr. Robert L. Walker for interesting discussions, and Dr. R. F. Bacher for his continued interest and encouragement.

PHYSICAL REVIEW VOLUME 107, NUMBER 2 JULY 15, 1957

Charge-Exchange Scattering of K^0 Beams as a Test of the Parity-Doublet Proposals*

HENRY P. STAPP
Radiation Laboratory, University of California, Berkeley, California
(Received February 11, 1957)

The determination of the $K_{3\pi}$ to $K_{2\pi}$ ratio in K^+ beams obtained from the charge-exchange scattering of a beam of neutral K-particles should resolve the question of whether the K-particle is a parity doublet or a single particle. In the parity-doublet case the $K_{3\pi}$ to $K_{2\pi}$ ratio would, in general, depend upon the scattering angle and would differ from the value obtained in ordinary K^+ beams. The value of the ratio would depend upon, and give information concerning, the specific form of the interaction. If the K-particle is assumed to have zero spin, and if the strong interactions are charge-independent and are invariant under time reversal as well as space reflection and parity conjugation, then the $K_{3\pi}$ to $K_{2\pi}$ ratio in either the forward elastically scattered beam or in the backward elastically scattered beam must be four times its normal value. If there is a $\pi-K$ interaction among these strong interactions, then it is the forward direction in which the $K_{3\pi}$ to $K_{2\pi}$ ratio is four times normal.

SECTION I

THE Dalitz analysis[1] indicates a parity difference in the reaction products of the two- and three-pion decay modes of the K-particle. Attempts to avoid the conclusion that parity is not conserved in this interaction have been advanced by several authors. Yang and Lee[2] have suggested that there may be two

* This work was performed under the auspices of the U. S. Atomic Energy Commission.

[1] R. Dalitz, *Proceedings of the Fifth Annual Rochester Conference on High-Energy Nuclear Physics, 1955* (Interscience Publishers, Inc., New York, 1955); R. Dalitz, *Proceedings of the Sixth Annual Rochester Conference on High-Energy Nuclear Physics, 1956* (Interscience Publishers, Inc., New York, 1956).

[2] T. D. Lee and C. N. Yang, Phys. Rev. **102**, 290 (1956). Since the completion of this note, some experiments suggested by Yang and Lee† have shown that parity is not conserved in interactions involving neutrinos. This result inclines one more strongly than